

# JOINT DECONVOLUTION OF FUNDAMENTAL AND HARMONIC ULTRASOUND IMAGES

Mohamad Hourani<sup>1,2</sup>, Adrian Basarab<sup>2</sup>, Denis Kouamé<sup>2</sup>, Jean-Yves Tourneret<sup>1</sup>

<sup>1</sup> University of Toulouse, IRIT/INP-ENSEEIH, 31071 Toulouse Cedex 7, France

<sup>2</sup> University of Toulouse, IRIT, CNRS UMR 5505, Université Paul Sabatier, Toulouse, France

{mohamad.hourani, adrian.basarab, denis.kouame}@irit.fr, {jean-yves.tourneret}@enseeiht.fr, {jmgirault}@univ-tours.fr,

## ABSTRACT

This paper studies the interest of using harmonic ultrasound (US) images in the process of tissue reflectivity function restoration from RF data. To this end, two direct models (one for fundamental and another for harmonic images) derived from the equation of US wave propagation are proposed. In particular, an axially varying attenuation matrix is used within the harmonic image model in order to account for the attenuation of harmonic echoes. Based on these two image formation models, a joint deconvolution problem is investigated. The solution of this problem is obtained by minimizing a cost function composed of two data fidelity terms representing the linear and non-linear model components, regularized by an  $\ell_1$ -norm regularization. The tissue reflectivity function minimizing this function is finally determined using an alternating direction method of multipliers. The performance of the proposed algorithm is quantitatively and qualitatively evaluated on synthetic data, and compared with a classical restoration method used for US images.

**Index Terms**— ultrasound imaging, harmonic ultrasound imaging, optimization, ADMM, joint deconvolution, image restoration.

## 1. INTRODUCTION

Among all medical imaging modalities, ultrasound (US) imaging is still the most used in clinics due to its effectiveness, non-ionizing and low cost characteristics [1]. It serves for clinical diagnosis, mainly for soft tissues such as cardiovascular applications, various cancer blood flow velocity assessment and obstetrics. US imaging refers to a pulse-echo technique where a brightness mode, called B-mode, is used to visualize the tissues. A short pulse with central frequency  $f_0$  is emitted by a transducer generating a US wave transmitted into the medium, reflected back to the probe by the scatterers. Radiofrequency (RF) signals are then produced by the echoes returning to the transducer. These raw RF signals are filtered around  $f_0$ , beamformed to generate RF lines and further juxtaposed, demodulated and log-compressed to form the fundamental B-mode image. US waves may interact non linearly with the medium during propagation causing distortion of the transmitted wave. This distortion introduces harmonic components into the spectrum of the received signals. Therefore, the received RF signals can be filtered around the harmonic components in order to obtain the so-called harmonic US images. For blood perfusion measurements and lesion characterization applications, contrast agents are injected to generate strong nonlinearities. However, existing studies showed that certain tissues can cause distortions without the need for contrast agents, enabling the so called tissue harmonic imaging (THI) [2]. Due to the limited bandwidth of the transducers, the study of US image harmonics is usually limited to the first component at  $2f_0$ . Several methods have been proposed to give access to both fundamental and harmonic images such as pulse

inversion [3], system identification [4] and filtering techniques in the case of low overlap between fundamental and harmonic spectra (see Fig. 1 for an illustrative example).

THI has several advantages over fundamental US imaging, such

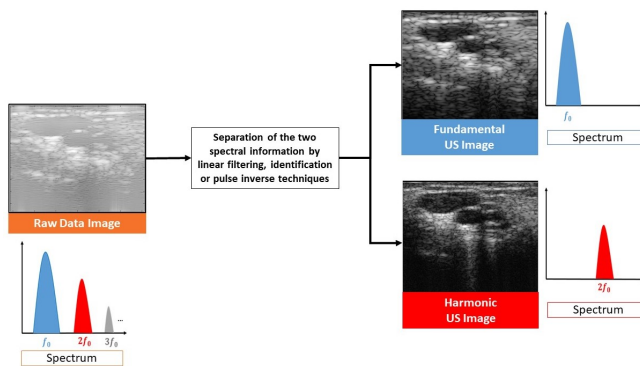


**Fig. 1.** Illustration of fundamental and harmonic images computed by linear filtering from the native RF image.

as better spatial resolution, improved contrast to noise ratio and reduced near field artifacts. However, the high attenuation with imaging depth is an important drawback. In US imaging, several attempts were proposed to increase the resolution and the contrast of the images by improving the beamformer, or restoring the tissue reflectivity function (TRF) by introducing appropriate post-processings on RF data (e.g., [5, 6]), which is the main objective of this work. More specifically, this paper accounts for harmonic US imaging in the process of TRF restoration, in addition to fundamental RF data.

The remainder of this paper is organized as follows: Section 2 summarizes the US propagation model and its linearization, justifying the US image models considered in Section 3. Section 4 shows how to solve the proposed deconvolution problem using an alternating direction method of multipliers (ADMM). Results on simulated data are presented in Section 5 whereas conclusion and future works are reported in Section 6.

## 2. PROBLEM STATEMENT

### 2.1. US image formation model

Under the first Born approximation, the full acoustic model allows the RF signal to be expressed as the convolution between a spatially varying pulse and the inhomogeneity of the field [7–9]. Thereby, convolution models are adapted in several ultrasound simulators (see e.g., [10, 11]). In ultrasound image restoration, this model is usually

simplified to the convolution with a spatially invariant PSF, restricting the restoration to image segments where this hypothesis roughly holds [12]. In this work we follow this trend and propose the following image formation models for fundamental and harmonic RF images

$$\mathbf{y}_f = \mathbf{H}_f \mathbf{r} + \mathbf{n}_f, \quad (1)$$

$$\mathbf{y}_h = \mathbf{W} \mathbf{H}_h \mathbf{r} + \mathbf{n}_h \quad (2)$$

where  $\mathbf{y}_f$  and  $\mathbf{y}_h \in \mathbb{R}^N$  are the observed fundamental and harmonic RF images,  $\mathbf{r} \in \mathbb{R}^N$  is the TRF to be estimated and  $\mathbf{n}_f$  and  $\mathbf{n}_h \in \mathbb{R}^N$  are white Gaussian additive noises with variances  $\sigma_f^2$  and  $\sigma_h^2$ .  $\mathbf{H}_f$  and  $\mathbf{H}_h \in \mathbb{R}^{N \times N}$  are block circulant with circulant blocks matrices accounting for the fundamental and harmonic system PSF and  $N$  is the number of image samples. Due to the attenuation of the harmonic image with depth, we consider in the second model a diagonal matrix  $\mathbf{W} \in \mathbb{R}^{N \times N}$  that accounts for the level of attenuation at each depth (the construction of this matrix will be explained later).

## 2.2. TRF estimation

The objective of this work is to estimate the TRF from the fundamental and harmonic RF signal, based on the direct models in (2). Using a Bayesian perspective, we propose to estimate the TRF using the standard MAP estimator, i.e., by minimizing the posterior distribution determines using Bayes rule as follows

$$p(\mathbf{r}|\mathbf{y}_f, \mathbf{y}_h) \propto p(\mathbf{y}_f|\mathbf{r})p(\mathbf{y}_h|\mathbf{r})p(\mathbf{r}) \quad (3)$$

where  $p(\mathbf{r})$  is the prior probability density function of  $\mathbf{r}$  and the two likelihood functions are given by:

$$\mathbf{y}_f|\mathbf{r}, \sim \mathcal{N}(\mathbf{H}_f \mathbf{r}, \sigma_f^2 \mathbf{I}_N) \quad (4)$$

$$\mathbf{y}_h|\mathbf{r}, \sim \mathcal{N}(\mathbf{W} \mathbf{H}_h \mathbf{r}, \sigma_h^2 \mathbf{I}_N)$$

where  $\mathbf{I}_N$  is the  $N \times N$  identity matrix and  $\mathcal{N}$  stands for the Gaussian distribution. Assuming independence between the two additive noises  $\mathbf{n}_f$  and  $\mathbf{n}_h$ , the negative log-posterior of  $\mathbf{r}$  can be obtained as

$$\begin{aligned} -\log p(\mathbf{r}|\mathbf{y}_f, \mathbf{y}_h) \propto & \underbrace{\frac{1}{2} \|\mathbf{y}_f - \mathbf{H}_f \mathbf{r}\|_2^2}_{\text{Fundamental data fidelity term}} + \underbrace{\frac{1}{2} \|\mathbf{y}_h - \mathbf{W} \mathbf{H}_h \mathbf{r}\|_2^2}_{\text{Harmonic data fidelity term}} \\ & + \underbrace{\log(p(\mathbf{r}))}_{\text{regularization}} \end{aligned} \quad (5)$$

In this work, we consider a Laplacian prior distribution  $p(\mathbf{r})$ , leading to an  $\ell_1$ -norm regularization term in the function to minimize (see, e.g., [13, 14] for a similar choice). Finally, the TRF image  $\mathbf{r}$  can be estimated by solving the following optimization problem

$$\min_{\mathbf{r}} \frac{1}{2} \|\mathbf{y}_f - \mathbf{H}_f \mathbf{r}\|_2^2 + \|\mathbf{y}_h - \mathbf{W} \mathbf{H}_h \mathbf{r}\|_2^2 + \mu \|\mathbf{r}\|_1 \quad (6)$$

where  $\mu$  is a hyperparameter weighting the contribution of the sparse regularization with respect to the two data fidelity terms.

## 3. OPTIMIZATION

To solve the joint deconvolution problem presented in the previous section, i.e., to determine the TRF from fundamental and harmonic RF images minimizing (6), we propose to use an algorithm based on the alternating direction method of multipliers (ADMM) [15, 16].

ADMM is a general optimization framework able to solve the following problem

$$\begin{aligned} \min_{\mathbf{u}, \mathbf{v}} \quad & f_1(\mathbf{u}) + f_2(\mathbf{v}) \\ \text{s.t.} \quad & \mathbf{A}\mathbf{u} + \mathbf{B}\mathbf{v} = \mathbf{c} \end{aligned} \quad (7)$$

where  $f_1$  and  $f_2$  are closed convex functions and  $\mathbf{A}, \mathbf{B}, \mathbf{u}, \mathbf{v}$  and  $\mathbf{c}$  are matrices and vectors of correct sizes. In order to adapt our problem to the ADMM framework, we rewrite (6) as follows

$$\begin{aligned} \min_{\mathbf{u}, \mathbf{v}} \quad & \frac{1}{2} \|\mathbf{y}_f - \mathbf{H}_f \mathbf{u}\|_2^2 + \frac{1}{2} \|\mathbf{y}_h - \mathbf{W} \mathbf{z}\|_2^2 + \mu \|\mathbf{w}\|_1 \quad (8) \\ \text{with} \quad & \begin{cases} f_1(\mathbf{u}) = \frac{1}{2} \|\mathbf{y}_f - \mathbf{H}_f \mathbf{u}\|_2^2 \\ f_2(\mathbf{v}) = \frac{1}{2} \|\mathbf{y}_h - \mathbf{W} \mathbf{z}\|_2^2 + \mu \|\mathbf{w}\|_1 \\ \mathbf{z} = \mathbf{H}_h \mathbf{r}, \mathbf{w} = \mathbf{u} = \mathbf{r} \\ \mathbf{v} = \begin{bmatrix} \mathbf{w} \\ \mathbf{z} \end{bmatrix} \end{cases} \text{ and } \begin{cases} \mathbf{A} = \begin{bmatrix} \mathbf{I}_N \\ \mathbf{H}_h \end{bmatrix} \\ \mathbf{B} = \begin{bmatrix} -\mathbf{I}_N & 0 \\ 0 & -\mathbf{I}_N \end{bmatrix} \\ \mathbf{c} = \mathbf{0}_N \end{cases} \end{aligned}$$

An iterative alternating minimization method over the variables  $\mathbf{u}$  and  $\mathbf{v}$  can then be applied to the augmented Lagrangian  $\mathcal{L}_A(\mathbf{u}, \mathbf{v}, \boldsymbol{\lambda})$  associated with (8) defined as

$$\mathcal{L}_A(\mathbf{u}, \mathbf{v}, \boldsymbol{\lambda}) = f_1(\mathbf{u}) + f_2(\mathbf{v}) + \frac{\beta}{2} \|\mathbf{A}\mathbf{u} + \mathbf{B}\mathbf{v}^k + \frac{\boldsymbol{\lambda}^k}{\beta}\|_2^2 \quad (9)$$

where  $\beta$  is a regularization parameter for the linear constraint, and  $\boldsymbol{\lambda} = \begin{bmatrix} \lambda_1 \\ \lambda_2 \end{bmatrix} \in \mathbb{R}^{2N}$  is the vector of Lagrangian multipliers. The solution of this problem can be iteratively obtained using 3 steps: estimate  $\mathbf{u}$ , estimate  $\mathbf{v}$  and update the Lagrangian vector  $\boldsymbol{\lambda}$ , as summarized in Algo. 1.

---

### Algorithm 1: ADMM algorithm for TRF estimation

---

**Input:**  $\mathbf{y}_f, \mathbf{y}_h, \mathbf{H}_f, \mathbf{H}_h$ .

1. Set  $k = 0$ , choose  $\mu > 0, \beta > 0, \mathbf{u}^0, \mathbf{v}^0$

2. Repeat until stopping criterion is satisfied

// Estimate  $\mathbf{u}$  (closed-form solution in the Fourier domain)

3.  $\mathbf{u}^{k+1} \in \min_{\mathbf{u}} \frac{1}{2} \|\mathbf{y}_f - \mathbf{H}_f \mathbf{u}\|_2^2 + \frac{\beta}{2} \|\mathbf{A}\mathbf{u} + \mathbf{B}\mathbf{v}^k + \frac{\boldsymbol{\lambda}^k}{\beta}\|_2^2$

// Estimate  $\mathbf{v} = \begin{bmatrix} \mathbf{w} \\ \mathbf{z} \end{bmatrix}$

// Estimate  $\mathbf{w}$  using soft thresholding

4.  $\mathbf{w}^{k+1} \in \min_{\mathbf{w}} \mu \|\mathbf{w}\|_1 + \frac{\beta}{2} \|\mathbf{u}^{k+1} - \mathbf{w} + \frac{\boldsymbol{\lambda}_1^k}{\beta}\|_2^2$

// Estimate  $\mathbf{z}$  (closed-form solution in the Fourier domain)

5.

$\mathbf{z}^{k+1} \in \min_{\mathbf{z}} \frac{1}{2} \|\mathbf{y}_h - \mathbf{W} \mathbf{z}\|_2^2 + \frac{\beta}{2} \|\mathbf{H}_h \mathbf{u}^{k+1} - \mathbf{z} + \frac{\boldsymbol{\lambda}_2^k}{\beta}\|_2^2$

// Update the Lagrangian multiplier

6.  $\boldsymbol{\lambda}^{k+1} = \boldsymbol{\lambda}^k + \beta(\mathbf{A}\mathbf{u}^{k+1} + \mathbf{B}\mathbf{v}^{k+1})$

---

## 4. SIMULATION RESULTS

The proposed joint deconvolution method was first tested on synthetic data. A controlled ground truth TRF was computed from a

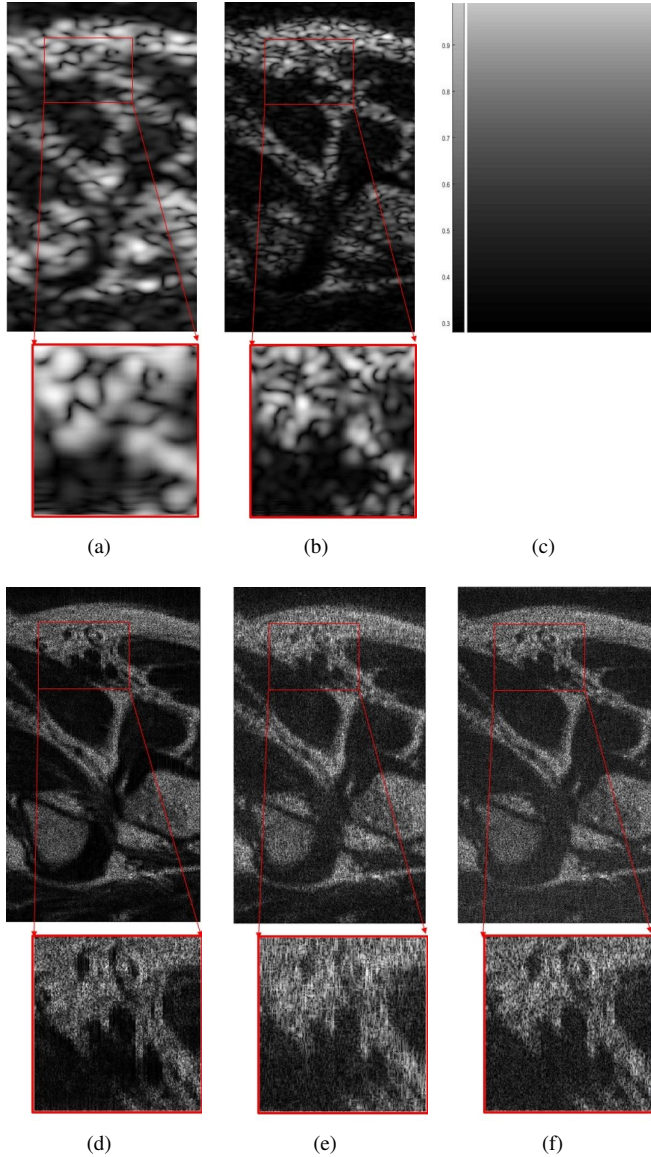


**Fig. 2.** (a) Simulated fundamental image  $y_f$ , (b) simulated harmonic image  $y_h$ , (c) attenuation map used to simulate the harmonic image in (b), whose values are equal to 1 (no attenuation) close to the probe and to 0.3 (high attenuation) at the bottom of the image, (d) TRF mimicking a human kidney ( $r$  of size  $1150 \times 300$  pixels), (e) TRF estimated by LASSO from the fundamental US image in (a), (f) TRF estimated by the proposed method from fundamental and harmonic US images in (a) et (b). Note that all the images are shown in B-mode for better visualisation.

slice of a kidney magnetic resonance image, by generating  $10^5$  scatterers with random Gaussian amplitudes. The size of the TRF image considered in this experiment was  $1150 \times 300$  pixels. Fundamental ( $y_f$ ) and harmonic ( $y_h$ ) RF images were then simulated by 2D convolution between the TRF and two spatially invariant PSFs  $H_f$  and  $H_h$ , with central frequencies of 3.5 MHz and 7 MHz respectively. The resulting images were contaminated with additive white Gaussian noise corresponding to an SNR of 50 dB. We notice that the algorithm can deal with higher noise level. The results obtained using the proposed algorithm were compared to the conventional de-

convolution problem where only the fundamental data fidelity term was considered. This classical method (referred to as LASSO) estimates the TRF by solving the following optimization problem

$$\min_r \frac{1}{2} \|y_f - H_f r\|_2^2 + \mu \|r\|_1. \quad (10)$$

To simulate the depth attenuation of the harmonic RF image, we use an exponential attenuation map shown in Fig. 2(c), corresponding to  $W$  in (6). The resulting fundamental and harmonic images are shown in Figs. 2(a) and (b). The original TRF and the estimated obtained using the proposed method and LASSO are shown in Figs. 2 (d), (e) and (f) respectively. Zooms corresponding to the red rectangle are also displayed for better visualization. A visual inspection of these TRF allows us to appreciate qualitatively the better accuracy of the proposed method compared to LASSO. To confirm these qualitative results, three quantitative measures of performance were computed between the estimated and true TRFs: the root mean square error (RMSE), the structural similarity index (SSIM) [17], and the improvement signal-to-noise ratio (ISNR) [18]. The results are provided in Table Tab. 4 showing clearly the interest of the proposed method compared to classical deconvolution.

	SSIM(%)	RMSE	ISNR(dB)
<b>Lasso</b>	63.95	0.0952	5.1116
<b>Proposed method</b>	<b>81.60</b>	<b>0.0635</b>	<b>8.6267</b>

**Table 1.** Quantitative results corresponding to the selected regions (in red) of images in Figs. 2(d), (e) and (f).

## 5. CONCLUSION

The objective of this work was to study the potential interest of considering a harmonic RF image in the process of TRF restoration in US imaging. Despite its high attenuation with depth and its low SNR, the harmonic image has a better spatial resolution than the fundamental image typically used in US image restoration. Combining this harmonic image with its fundamental counterpart provides interesting deconvolution results taking into account the properties of both images. Future works will be devoted to apply the proposed approach to *in vivo* data with a non-supervised approach. In this case, the problem can be formulated as a blind deconvolution problem into which a PSF estimation step has to be implemented either in a pre-processing step or jointly with the TRF estimation. Considering a spatially varying PSF in order to better match the direct models to practical situations is also an interesting prospect.

## 6. REFERENCES

- [1] T. L. Szabo, *Diagnostic ultrasound imaging: inside out*. Academic Press, San Diego, California, 2004.
- [2] M. A. Averkiou, D. N. Roundhill, and J. E. Powers, "A new imaging technique based on the nonlinear properties of tissues," *IEEE Ultrason. Symp. (US)*, vol. 2, pp. 1561–1566, 1997.
- [3] D. H. Simpson, C. T. Chin, and P. N. Burns, "Pulse inversion doppler: a new method for detecting nonlinear echoes from microbubble contrast agents," *IEEE Trans. Ultrason. Ferroelectr. Freq. Control*, vol. 46, no. 2, pp. 372–382, 1999.
- [4] A. Novak, L. Simon, F. Kadlec, and P. Lotton, "Nonlinear system identification using exponential swept-sine signal," *IEEE Trans. Instrum. Meas.*, vol. 59, no. 8, pp. 2220–2229, 2010.

- [5] O. V. Michailovich and D. Adam, "A novel approach to the 2-d blind deconvolution problem in medical ultrasound," *IEEE Trans. Med. Imag.*, vol. 24, no. 1, pp. 86–104, 2005.
- [6] T. Taxt, "Restoration of medical ultrasound images using two-dimensional homomorphic deconvolution," *IEEE Trans. Ultrason. Ferroelect., Freq. Control*, vol. 42, no. 4, pp. 543–554, 1995.
- [7] J. Ng, R. Prager, N. Kingsbury, G. Treece, and A. Gee, "Modeling ultrasound imaging as a linear, shift-variant system," *IEEE Trans. Ultrason. Ferroelect. Freq. Control*, vol. 53, no. 3, pp. 549–563, 2006.
- [8] J. A. Jensen, "Field: A program for simulating ultrasound systems," in *Med. Biol. Eng. Comput.*, , vol. 34, Supplement 1, Part 1: 351–353, 1996.
- [9] J. A. Jensen and N. B. Svendsen, "Calculation of pressure fields from arbitrarily shaped, apodized, and excited ultrasound transducers," *IEEE Trans. Ultrason. Ferroelect. Freq. Control*, vol. 39, no. 2, pp. 262–267, 1992.
- [10] H. Gao, H. F. Choi, P. Claus, S. Boonen, S. Jaecques, G. H. Van Lenthe, G. Van der Perre, W. Lauriks, and J. D'hooge, "A fast convolution-based methodology to simulate 2-d/3-d cardiac ultrasound images," *IEEE Trans. Ultrason. Ferroelect. Freq. Control*, vol. 56, no. 2, pp. 404–409, 2009.
- [11] A. Marion, J. Porée, and D. Vray, "Creasimus: a fast simulator of ultrasound image sequences using 3d tissue motion," in *IEEE Int. Ultrason. Symp.* IEEE, 2009, pp. 2308–2311.
- [12] J.-P. Ardouin and A. Venetsanopoulos, "Modelling and restoration of ultrasonic phased-array b-scan images," *Ultrasonic imaging*, vol. 7, no. 4, pp. 321–344, 1985.
- [13] R. Morin, S. Bidon, A. Basarab, and D. Kouamé, "Semi-blind deconvolution for resolution enhancement in ultrasound imaging," in *IEEE Proc. Int. Conf. Image Process. (ICIP)*, Melbourne, Australia, Feb. 2013.
- [14] Z. Chen, A. Basarab, and D. Kouamé, "Compressive deconvolution in medical ultrasound imaging," *IEEE Trans. Med. Imag.*, vol. 35, no. 3, pp. 728–737, 2016.
- [15] D. Gabay and B. Mercier, "A dual algorithm for the solution of nonlinear variational problems via finite element approximation," *Computers & Mathematics with Applications*, vol. 2, no. 1, pp. 17–40, 1976.
- [16] S. Boyd, N. Parikh, E. Chu, B. Peleato, and J. Eckstein, "Distributed optimization and statistical learning via the alternating direction method of multipliers," *Foundations and Trends in Machine Learning*, vol. 3, no. 1, pp. 1–122, 2011.
- [17] Z. Wang, A. C. Bovik, H. R. Sheikh, and E. P. Simoncelli, "Image quality assessment: from error visibility to structural similarity," *IEEE Trans. Image Process.*, vol. 13, no. 4, pp. 600–612, 2004.
- [18] S. Jayaramam, S. Esakkirajan, and T. Veerakumar, *Digital Image Processing*. Tata McGraw-Hill Education, 2011.